UDC 621.315.592

GaP_xAs_{1-x} solid solution growth by molecular beam epitaxy: phenomenological description of the x dependence from growth conditions on GaAs(001) substrate

© M.A. Putyato, E.A. Emelyanov¶, M.O. Petrushkov, A.V. Vasev, B.R. Semyagin, V.V. Preobrazhenskii

Rzhanov Institute of Semiconductor Physics, Siberian Branch, Russian Academy of Sciences,
630090 Novosibirsk, Russia

¶ E-mail: e2a@isp.nsc.ru

Received October 14, 2022
Revised January 31, 2023
Accepted February 23, 2023

The experimental dependences of the GaP_xAs_{1-x} solid solution phosphorus proportion on growth conditions by molecular beam epitaxy from As_2 and P_2 molecules on GaAs(001) substrate were described using the phenomenological model. The model was built on the well-established ideas about the III−V compounds MBE growth. The ratio of the arsenic and phosphorus atoms incorporation coefficients was considered as a function of the substrate temperature and molecular flux densitys. Empirical expressions were found that describe the behavior of the arsenic and phosphorus incorporation coefficients ratio depending on the indicated growth parameters. This makes it possible to estimate the V group molecule flux values to obtain the required x in a GaP_xAs_{1-x} solid solution at the given substrate temperature and the gallium atoms flow density.

Keywords: molecular beam epitaxy, $A^{III}B^{V}$, solid solutions, GaP_xAs_{1-x}, phenomenological model.

DOI: 10.21883/SC.2023.02.55949.4225

1. Introduction

Solid solutions $(A^{III})P_xAs_{1-x}$ feature a unique combination of properties that make them suitable for a most extensive range of applications in band engineering [1]. For example, varying x and y in $In_yGa_{1-y}P_xAs_{1-x}$, one may adjust independently the bandgap width and the lattice parameter of this material. The bandgap width of the quaternary solution varies from 1.42 to 1.90 eV in a matched $In_yGa_{1-y}P_xAs_{1-x}$/GaAs system and from 0.70 to 1.35 eV in $In_yGa_{1-y}P_xAs_{1-x}$/InP. Since compound $In_yGa_{1-y}P_xAs_{1-x}$ retains the characteristics of a direct-gap semiconductor within almost the entire range of compositions, it is suitable for the design of optoelectronic devices. Heterosystems mismatched in the lattice parameter (e.g., GaP_xAs_{1-x}/GaAs) are also of interest. Photocathodes generating a flux of spin-polarized electrons are fabricated based on strained GaP_xAs_{1-x}/GaAs superlattices. The degree of polarization of electrons in such devices reaches 92% at a quantum yield of $\sim 0.5\%$ [2]. Strained superlattices are formed on relaxed buffer GaP_xAs_{1-x} layers grown on GaAs substrates.

Various methods, including molecular beam epitaxy (MBE), are used to grow structures containing $(A^{III})P_xAs_{1-x}$ layers. The composition in the cation sublattice of an epitaxial layer in MBE of $(A^{III})P_xAs_{1-x}$ solid solutions is specified unambiguously by the flux densities of atoms of group III elements. The composition in the sublattice of group V depends in a complex way on the substrate temperature (T_s), the magnitude and the ratio of fluxes of molecules of group V elements and group III atoms (J_V and J_{III}), the composition and the surface state of a solid solution in the process of epitaxy, the molecular form of group V elements in the flux, and the crystallographic orientation of the substrate surface [3–7]. When working out the procedure of growth of heterostructures containing layers of $(A^{III})P_xAs_{1-x}$ solid solutions, one is faced with the problem of adjusting the flux densities of arsenic and phosphorus molecules to achieve the needed x value under the chosen epitaxy conditions. This problem is solved by growing test samples, determining the composition of obtained films, and correcting the ratio of fluxes as needed. While this approach is time- and material-consuming, it still remains relevant. The key reasons for this are as follows. First, it is reliable. Second, the methods for *in situ* controlling the proportion of phosphorus (arsenic) proposed in literature have certain limitations in regard to the epitaxy conditions [8–10]. Third, no techniques for *a priori* estimation of the flux densities of group V molecules needed to achieve the required x value within a wide range of growth conditions are available. It is by no means easy to develop such a technique.

A considerable amount of experimental data on MBE growth of $(A^{III})P_xAs_{1-x}$ solid solutions has been accumulated in literature. However, the lack of consistent approaches both to measurement of the molecular flux densities of group V elements and T_s and to presentation of results of such measurements makes it hard to perform a comparative analysis of the results of studies reported by different research groups. In addition, contradictory data regarding the influence of T_s in the process of MBE on the composition of GaP_xAs_{1-x} solid solutions are found in

literature. It was demonstrated in [11] that the proportion of phosphorus in a GaP_xAs_{1-x} solid solution decreases with increasing T_s. According to the results of other studies, the proportion of phosphorus in a solid solution is either unaffected by the substrate temperature [12] or increases with T_s [13]. The methodological incoherence and sparseness of the combined set of experimental data make it hard to piece together a consistent pattern of influence of MBE growth conditions on the composition of $(A^{III})P_xAs_{1-x}$ solid solutions. This is the reason why the available relatively simple steady-state kinetic models of growth of GaP_xAs_{1-x} solid solutions are limited in regard to the range of growth conditions. A more complex model, which takes into account non-steady processes occurring on the surface in the 2D layer growth regime, has been formulated based on experimental data in our earlier study [14]. The used experimental data cover a wide range of epitaxy conditions and were obtained within a consistent methodological approach to determination and control of the growth parameters. The model provides an adequate fit to the experimental data from [14] and makes it possible to resolve the discrepancies regarding the influence of temperature that are found in scientific literature. However, this model is mostly a tool for analysis of processes and growth mechanisms in MBE of $(A^{III})P_xAs_{1-x}$ solid solutions. A simpler model is needed for practical applications. A phenomenological approach, which does not require additional assumptions and a detailed examination of the mechanisms underlying experimental dependences, appears to be promising in this context. However, it is questionable whether such an approach is adequate to the task of characterizing the dependence of x on MBE parameters within a wide range of their values. This needs to be verified in the case of a typical $(A^{III})P_xAs_{1-x}$ solid solution. In the present study, phenomenological analysis of experimental dependences of the proportion of phosphorus in a GaP_xAs_{1-x} solid solution on the conditions of MBE on GaAs(001) substrates with As_2 and P_2 molecular fluxes is performed. Experimental data from [14] and the results obtained in the present study were used in the analysis.

2. Experiment

Samples with a GaP_xAs_{1-x} solid solution were grown on GaAs substrates with a 0.1° deviation from the (001) face in direction [110]. The growth parameters varied within the following ranges: T_s, from 400 to 600°C; V_g, from 0.25 to 2.5 μm per hour; ratio $2J_{As_2}/J_{Ga}$, from 0.5 to 10; and ratio $2J_{P_2}/J_{Ga}$, from 1 to 16. Fluxes of As_2 and P_2 molecules were used. The ranges of variation of growth parameters of samples do not overlap with the regions of existence of interphase transitions between surface structures (SS) in state diagrams that characterize the surface state in the process of growth. As was already noted, GaP_xAs_{1-x} is mismatched in the lattice parameter with GaAs. This mismatch becomes more pronounced as x increases. When a growing GaP_xAs_{1-x} film reaches a critical thickness, the process of its plastic relaxation with the introduction of mismatch dislocations is initiated. In the present case, all films of solid solutions had an above-critical thickness and relaxed within 3–80% depending on their composition and thickness. The growth conditions of samples were detailed in [14].

The values of fluxes of group V molecules used in model calculations were determined based on the ion currents of an ion gage head introduced in measurements into direct fluxes to the substrate position. The mean relative deviation from the initial flux value for both elements is $\delta_J \approx \pm 5.5\%$.

The drift of density of molecular fluxes of group V elements in the process of growth translates into a certain compositional nonuniformity of the solid solution over the thickness of epitaxial films. The prepared samples were subjected to X-ray diffraction analysis, which provided an opportunity to determine fairly accurately the composition of the solid solution averaged over the film thickness.

3. Description of the model

The model is based on universally accepted and experimentally verified concepts of MBE of $A^{III}B^V$ compounds. Atom incorporation coefficients S were used to characterize the balance of mass transfer processes in MBE of $A^{III}B^V$ compounds. Coefficient S was defined as the ratio of the number of atoms incorporated into the crystal lattice of an epitaxial film within a certain period of time to the number of atoms in a certain molecular form incident onto the surface within the same period of time. Under typical epitaxy conditions, the incorporation coefficient of group III atoms is equal to unity. Therefore, the composition of solid solutions in the cation sublattice is defined unambiguously by the ratio of fluxes of metal atoms. A different pattern is observed in the production of solid solutions by substitution by group V. The incorporation coefficient of molecules of group V elements are lower than unity, depend on the growth conditions, and differ significantly between themselves. Therefore, the composition of a solid solution with substitution in the anion sublattice depends in a complex way on the growth conditions.

The proportion of phosphorus (x) in MBE of GaP_xAs_{1-x} solid solutions from fluxes of As_2 and P_2 molecules is related to the flux densities of group V elements in the following way:

$$x = \frac{J_{P_2} \times S_{P_2}}{J_{P_2} \times S_{P_2} + J_{As_2} \times S_{AS_2}} = \frac{1}{1 + \frac{J_{As_2}}{J_{P_2}} \times R_s}, \quad (1)$$

where J_{As_2} and J_{P_2} are the flux densities of As_2 and P_2 molecules, S_{As_2} and S_{P_2} are the incorporation coefficients of arsenic and phosphorus atoms with As_2 and P_2 molecules used in the process, and $R_s = S_{As_2}/S_{P_2}$. One needs to know

the value of R_s to estimate the composition of the solid solution using expression (1) at a given J_{As_2}/J_{P_2}.

Parameter R_s depends in a complex way on T_s, J_{As_2}, J_{P_2}, the flux density of gallium atoms (J_{Ga}), and other growth parameters, including the surface state of the solid solution in the process of epitaxy. The surface state is characterized by the SS and its defects and the concentration of chemisorption sites for molecules of group V elements established by incorporating gallium atoms. It is important to note that the surface state is specified by T_s, J_{As_2}, J_{P_2}, J_{Ga}, and, in particular, ratio J_V/J_{Ga} of the fluxes of group V molecules and group III atoms. Therefore parameter R_s was regarded within our phenomenological approach as a function of T_s, $X = 2J_{P_2}/J_{Ga}$, and $Y = 2J_{As_2}/J_{Ga}$ (under otherwise equal conditions): $R_s = R(X, Y, T_s)$.

4. Approximation analysis of the experimental dependences of R_s on the growth conditions

The behavior of R_s as a function of the growth conditions was analyzed without examining the probable internal mechanisms underlying the analyzed regularities. The simplest functions providing an adequate approximation of experimental dependences were chosen in the process of analysis. Approximating functions were identified with the use of the Origin software for numerical data analysis and scientific graphing. Expressions for calculating R_s based on the known values of J_{As_2}, J_{P_2}, J_{Ga}, and T_s were derived using the chosen functions. The initial values of coefficients of approximating functions determined in Origin were subsequently corrected in MathCAD (a mathematical software package) by minimizing the deviation between calculated and experimental data.

It was demonstrated in [3,4,12] that the composition of a GaP_xAs_{1-x} solid solution may be controlled efficiently by varying J_{As_2} under otherwise constant growth conditions. This approach is technologically convenient. Two structures with a step change of the proportion of phosphorus in layers of a GaP_xAs_{1-x} solid solution were grown under this approach. The growth temperature was 480°C, and $J_{Ga} = 6.14 \cdot 10^{14}\,\mathrm{cm}^{-2} \cdot \mathrm{c}^{-1}$. Ratio $2J_{P_2}/J_{Ga} \approx 16$ was set to suppress the influence of effects induced by the SS rearrangement due to J_{As_2} reduction. The layer composition was determined via layer-by-layer Auger spectroscopy. Figure 1 shows the dependence of the proportion of phosphorus in a GaP_xAs_{1-x} solid solution on ratio J_{As_2}/J_{P_2}. Expression (1) at $R_s = 9.6$ (solid curve) provides an adequate fit to experimental x values (triangles).

Figure 2 presents the dependences of incorporation coefficients S_{As_2} and S_{P_2} on $2J_{As_2}/J_{Ga}$. Dashed curves are approximations of experimental data with a function of the following form: $y = a + b\exp(-x/c)$. This function produces a monotonic curve providing an adequate fit to experimental data. It should be noted that approximating functions were chosen here and elsewhere for their simplicity and accuracy of data interpolation rather than on the basis of assumptions regarding the mechanisms of interaction of atoms and molecules with the surface.

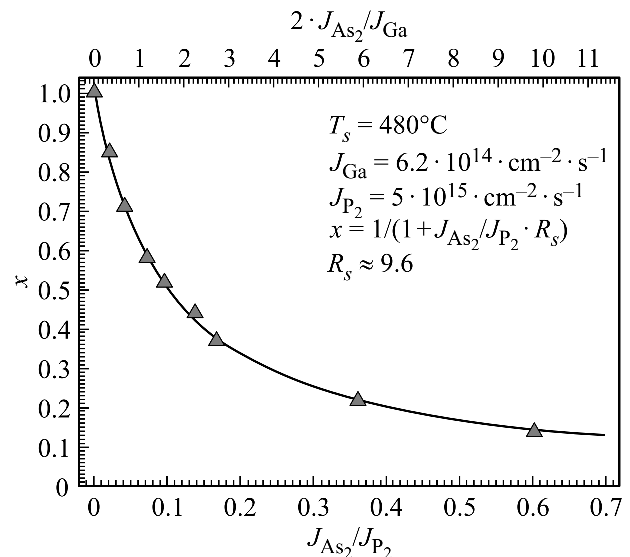

Figure 1. Dependence of the proportion of phosphorus in a GaP_xAs_{1-x} solid solution on ratio J_{As_2}/J_{P_2}. Triangles represent experimental data, and the solid curve is the result of approximation with expression (1).

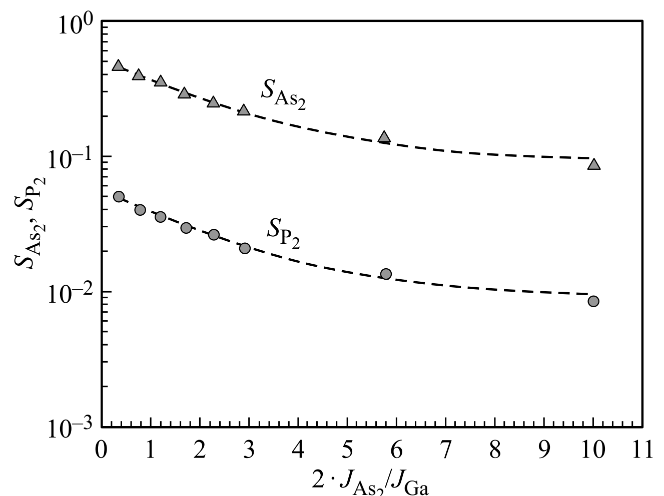

Figure 2. Experimental dependences of S_{As_2} (triangles) and S_{P_2} (circles) on $2J_{As_2}/J_{Ga}$ in the process of MBE of a GaP_xAs_{1-x} solid solution. Dashed curves represent the result of approximation with a function of the following form: $a + b\exp(-x/c)$.

It follows from the dependences in Fig. 2 that the incorporation coefficients of arsenic and phosphorus decrease almost equidistantly. As a result, R_s varies just from 9.2 to 10.2 as ratio $2J_{As_2}/J_{Ga}$ increases from 0.32 to 10.

Three series of samples with single GaP_xAs_{1-x} layers from [14] were examined in order to clarify the nature of functional relation between R_s and J_V/J_{III}. Films were grown at T_s = 550, 500, and 400°C. The gallium flux

density was $6.26 \cdot 10^{14}\,\mathrm{cm}^{-2} \cdot \mathrm{c}^{-1}$ in all cases. The fluxes of As_2 and P_2 molecules were varied from one sample to the other within each series in such a way that ratio J_{As_2}/J_{P_2} remained unchanged. Figure 3 shows the dependences of R_s on $2(J_{As_2} + J_{P_2})/J_{Ga}$. It follows from these plots that a reduction in $2(J_{As_2} + J_{P_2})/J_{Ga}$ leads to a reduction in R_s and the dependence of R_s on $2(J_{As_2} + J_{P_2})/J_{Ga}$ grows stronger in the process. As T_s decreases, the influence of ratio $2(J_{As_2} + J_{P_2})/J_{Ga}$ on R_s becomes more pronounced.

Two series of GaP_xAs_{1-x} films [14] were grown to determine the nature and the extent of influence of ratios $2J_{As_2}/J_{Ga}$ and $2J_{P_2}/J_{Ga}$ on R_s. The first series was fabricated at $2J_{P_2}/J_{Ga} = \mathrm{const}$ and different values of ratio $2J_{As_2}/J_{Ga}$, and the second one was formed at

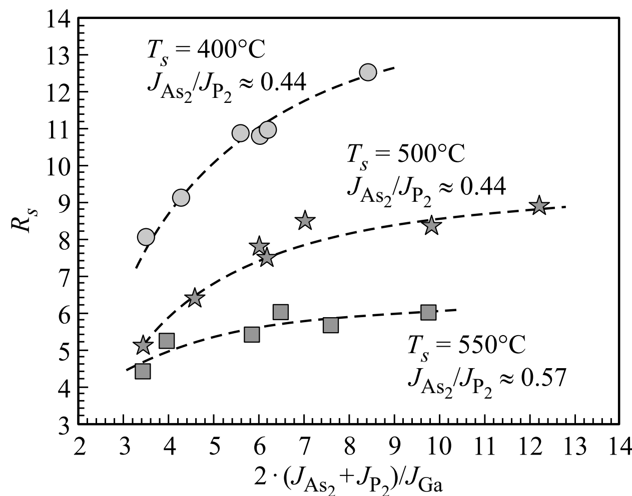

Figure 3. Experimental dependences of R_s on $2(J_{As_2} + J_{P_2})/J_{Ga}$ during MBE of GaP_xAs_{1-x} solid solution at different values of T_s. Dashed curves represent the result of approximation with a function of the following form: $a + b\exp(-x/c)$.

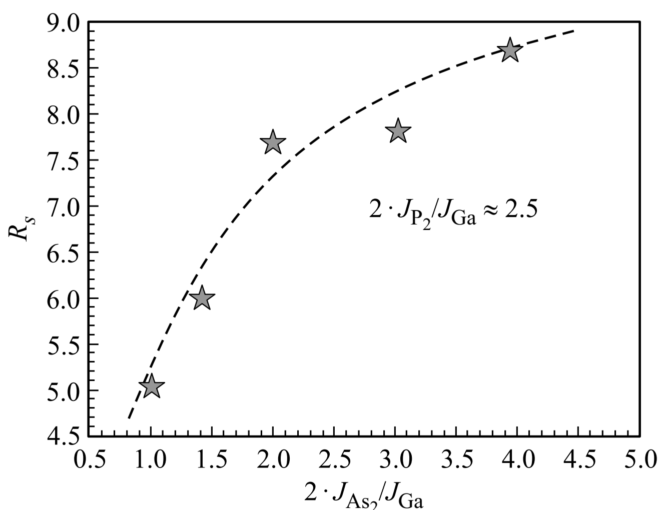

Figure 4. Dependence of S_{As_2}/S_{P_2} on $2J_{As_2}/J_{Ga}$ in the process of MBE of a GaP_xAs_{1-x} solid solution. $2J_{P_2}/J_{Ga} \approx 2.5$, $J_{Ga} = 6.26 \cdot 10^{14}\,\mathrm{cm}^{-2} \cdot \mathrm{c}^{-1}$, $T_s = 500$°C.

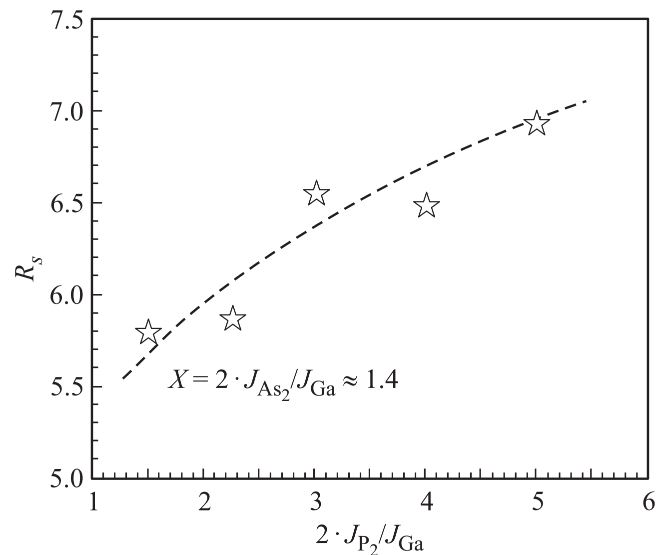

Figure 5. Dependence of S_{As_2}/S_{P_2} on $2J_{As_2}/J_{Ga}$ in the process of MBE of a GaP_xAs_{1-x} solid solution. $2J_{P_2}/J_{Ga} \approx 2.5$, $J_{Ga} = 6.26 \cdot 10^{14}\,\mathrm{cm}^{-2} \cdot \mathrm{c}^{-1}$, $T_s = 500$°C.

$2J_{As_2}/J_{Ga} = \mathrm{const}$ and varying values of $2J_{P_2}/J_{Ga}$. All samples were grown at $J_{Ga} = 6.26 \cdot 10^{14}\,\mathrm{cm}^{-2} \cdot \mathrm{c}^{-1}$ and $T_S = 500$°C. Figures 4 and 5 present the obtained dependences of R_s on $2J_{As_2}/J_{Ga}$ and $2J_{P_2}/J_{Ga}$, respectively. Ratio R_s decreases with decreasing $2J_{P_2}/J_{Ga}$ and $2J_{As_2}/J_{Ga}$, and the influence of $2J_{P_2}/J_{Ga}$ and $2J_{As_2}/J_{Ga}$ on R_s grows stronger in the process. It follows from the dependences shown in Figs. 4 and 5 that the variation of $2J_{As_2}/J_{Ga}$ exerts a significantly more pronounced effect on R_s than $2J_{P_2}/J_{Ga}$ within the region of $2J_{P_2}/J_{Ga}$ and $2J_{As_2}/J_{Ga}$ values from 1 to 2.5.

A comparative analysis of the dependences in Figs. 3, 4–5 revealed that the behavior of ratio R_s at $T_s = 500$°C and $J_{Ga} \approx 6.26 \cdot 10^{14}\,\mathrm{cm}^{-2} \cdot \mathrm{c}^{-1}$ is characterized adequately by the following expression:

$$Rs_{500^\circ\mathrm{C}} = a - b\exp\left(-\frac{2J_{As_2}}{J_{Ga}c}\right),$$

$$a = 9.40 + 0.03\,\frac{2J_{P_2}}{J_{Ga}},$$

$$b = 1.50 + 14.00\exp\left(-\frac{2J_{P_2}}{4.21J_{Ga}}\right),$$

$$c = 0.98 + 0.08\,\frac{2J_{P_2}}{J_{Ga}}. \qquad (2)$$

The foregoing suggests that a reduction in J_{Ga} within a certain surface structure should lead to an increase in R_s, since ratios $2J_{As_2}/J_{Ga}$ and $2J_{P_2}/J_{Ga}$ increase in this case. No literature data on the influence of J_{Ga} on the composition of GaP_xAs_{1-x} formed by solid-source MBE have been found. A series of samples were grown at $T_s = 500$°C and $J_{As_2}/J_{P_2} \approx 0.53$ in order to determine the

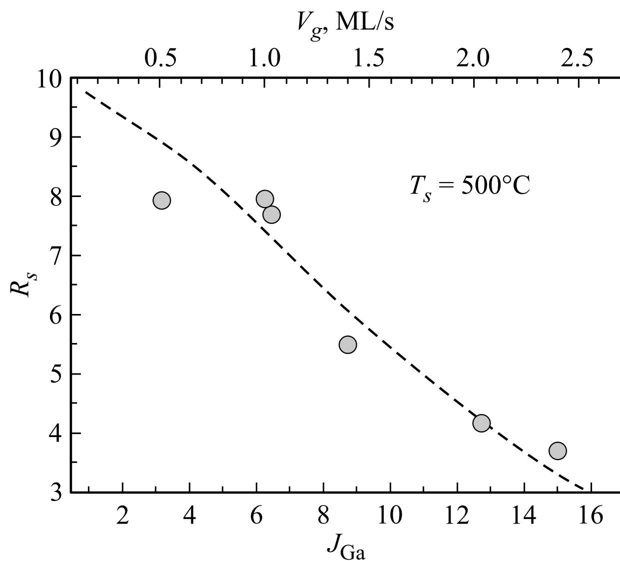

Figure 6. Dependence of R_s on J_{Ga} (and growth rate V_g corresponding to flux density J_{Ga}) in the process of MBE of a GaP_xAs_{1-x} solid solution. Circles denote experimental data. The dashed curve is the dependence of R_s on J_{Ga} plotted using approximation (2) at $J_{As_2}/J_{P_2} = 0.63$ and $J_{P_2} = 1.9 \cdot 10^{15}\,cm^{-2} \cdot c^{-1}$.

nature of the dependence of the solid solution composition on J_{Ga} [14]. The gallium flux density was varied from $1.5 \cdot 10^{14}$ to $1.5 \cdot 10^{15}\,cm^{-2} \cdot c^{-1}$. Figure 6 presents the experimental data on the dependence of R_s on J_{Ga} (circles) and the dependence of R_s on J_{Ga} plotted using approximating relation (2) (dashed curve).

The experimental values of R_s vary nonmonotonically within the considered range of J_{Ga} values. The point of change in the nature of the dependence corresponds to a gallium flux density $\approx 4.5 \cdot 10^{14}\,cm^{-2} \cdot c^{-1}$. It is unexpected that ratio R_s decreases as the gallium flux density drops below a certain threshold. Approximation (2) yields an inadequate estimate of R_s in the region of low growth rates (see the dashed curve in Fig. 6). It should be noted that the model discussed in [14] provides an adequate description of the behavior of R_s within this range of growth rates.

When analyzing literature data on the influence of the growth temperature on the composition of a GaP_xAs_{1-x} solid solution, one is faced with the problem of matching of the results of T_s measurements reported in different studies. In many scenarios, a solution to this problem with a desired degree of reliability remains elusive. This is the reason why experiments aimed at clarifying the nature of influence of the growth temperature on the incorporation of arsenic and phosphorus in the process of MBE of a GaP_xAs_{1-x} solid solution were performed in [14]. A series of samples with single layers of a GaP_xAs_{1-x} solid solution were grown for this purpose at different T_s values ranging from 400 to 600°C. The gallium flux density was $6.26 \cdot 10^{14}\,cm^{-2} \cdot c^{-1}$. The obtained data were split into three groups corresponding to different mean values of $2J_{As_2}/J_{Ga}$. The J_{As_2}/J_{P_2} ratio varied insignificantly within each of these groups. The obtained dependences of ratio R_s on T_s are presented in Fig. 7.

Symbols (circles, squares, and triangles) denote experimental data. The approximating functions are quadratic polynomials. These dependences demonstrate that the relative efficiency of arsenic incorporation decreases with increasing T_s. As $2J_{As_2}/J_{Ga}$ goes down, the temperature dependence of R_s grows weaker.

Figure 8 shows the dependence of the proportion of phosphorus (x) in a GaP_xAs_{1-x} solid solution on T_s taken from [14]. It follows from the analysis of this

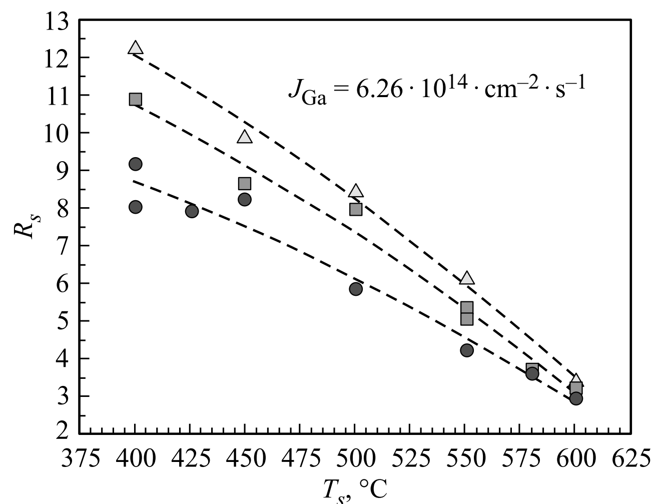

Figure 7. Dependence of ratio R_s on T_s in the process of MBE of a GaP_xAs_{1-x} solid solution. Circles, squares, and triangles denote experimental data obtained at $2J_{As_2}/J_{Ga} \approx 1.35$, $2J_{As_2}/J_{Ga} \approx 1.6$, and $2J_{As_2}/J_{Ga} \approx 2.2$, respectively.

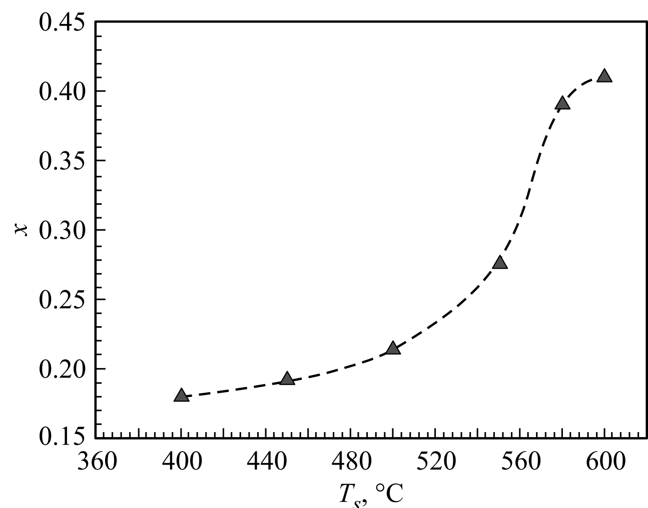

Figure 8. Dependence of the proportion of phosphorus (x) in a GaP_xAs_{1-x} solid solution on T_s. Data were obtained at $J_{Ga} = 6.26 \cdot 10^{14}\,cm^{-2} \cdot c^{-1}$, $J_{As_2}/J_{Ga} \approx 1.6$, and $J_{As_2}/J_{P_2} \approx 0.44$. The dashed curve was drawn for clarity.

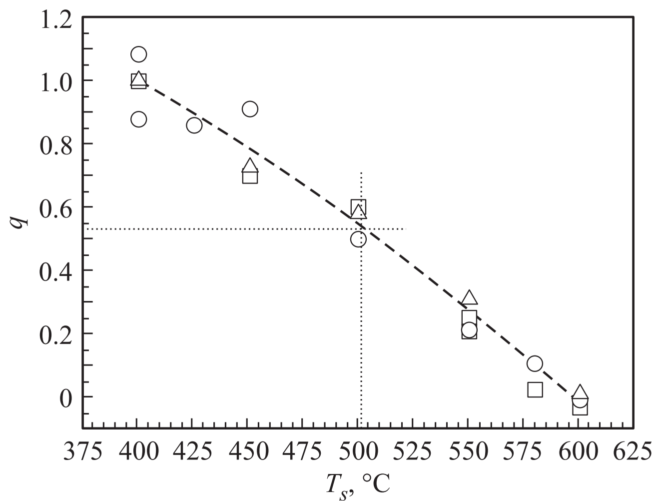

Figure 9. Dependence of q (see expression (3)) on T_s. Circles, triangles, and squares denote the values calculated based on experimental data at $2J_{As_2}/J_{Ga} \approx 1.35$, and $2J_{As_2}/J_{Ga} \approx 2.2$, respectively. $2J_{As_2}/J_{Ga} \approx 1.6$,

dependence that parameter x varies relatively weakly with growth temperature in the region of low T_S values. At $500 < T_S < 580$°C, the growth temperature exerts a considerable influence on the proportion of phosphorus in a solid solution. The influence of substrate temperature on the composition of a GaP_xAs_{1-x} solid solution grows weaker again in the region of $T_s > 580$°C.

The presented temperature dependences of x and R_s agree qualitatively with the results reported in [13], but contradict formally the data from [11], where an increase in the substrate temperature led to an enhancement of S_{As_4}/S_{P_4} (in the process of epitaxy of a GaP_xAs_{1-x} solid solution from As_4 and P_4 fluxes). This discrepancy is addressed in the Discussion section.

The obtained data provided an opportunity to construct an empirical expression for estimating the influence of T_S on the composition of a GaP_xAs_{1-x} solid solution based on a known value of R_s at 500°C (see expression (2)). The dependences of R_s on T_s (Fig. 7) were analyzed for this purpose. It was found that the values of parameter q, which is given by

$$q = \frac{Rs - Rs_{600^\circ C}}{Rs_{400^\circ C} - Rs_{600^\circ C}}, \tag{3}$$

for all dependences within the range of $2J_{As_2}/J_{Ga}$ from 1.35 to 2.2 (see Fig. 9) are equal with a sufficient accuracy. At $T_s = 500$°C, $q_{500^\circ C} \approx 0.53$. The value of $Rs_{600^\circ C}$ may be set to 3.25 for all dependences of R_s on T_s within the range of $2J_{As_2}/J_{Ga}$ values from 1.35 to 2.2 (see Fig. 7).

If the value of $Rs_{500^\circ C}$ is known, one may determine $Rs_{400^\circ C}$:

$$Rs_{400^\circ C} = \frac{Rs_{500^\circ C} - Rs_{600^\circ C}}{q_{500^\circ C}} + Rs_{600^\circ C}. \tag{4}$$

If $Rs_{400^\circ C}$, $Rs_{600^\circ C}$, and q are known, the value of R_s for any temperature from 400 to 600°C may be determined using Eq. (3). The expression for calculation of q takes the form

$$q = 1.73 + 6.78 \cdot 10^{-4} T_S - 5.96 \cdot 10^{-6} T_S^2. \tag{5}$$

It should be stressed that expressions (2)−(5) are not representative in their form or structure of the physical nature of the relation between ratio R_s and the growth conditions, but allow one to estimate, with the help of expression (1) that has a clear physical interpretation, the composition of a GaP_xAs_{1-x} solid solution based on known values of J_{As_2}, J_{P_2}, J_{Ga}, and T_s. This simplifies the task of experimental adjustment of arsenic and phosphorus fluxes performed to reach a given proportion of phosphorus x.

5. Numerical description of experimental data

Experimental dependences of the proportion of phosphorus in a GaP_xAs_{1-x} solid solution on MBE conditions were approximated using expression (1) (with expressions (2)−(5) taken into account) in MathCAD. The results were validated by comparing calculated x_c and experimental x_e proportions of phosphorus in a solid solution. The initial values of coefficients of approximating functions determined in Origin were corrected by minimizing the discrepancy between x_c and x_e.

5.1. Criteria for evaluation of validity of the model

Arithmetic mean values δ_{DT} of absolute deviations of x_c from x_e for several T_s ranges:

$$\delta_{DT} = \frac{1}{p} \sum_{j=1}^{p} \left| \frac{x_{cj} - x_{ej}}{x_{ej}} \right|, \tag{6}$$

where p is the number of samples within range DT, served as the quantitative criterion for evaluation of validity of the model in regard to the temperature dependence.

In order to refine the validity estimate of the model, arithmetic mean values δ_T of absolute deviations of x_c from x_e were calculated within groups with a fixed T_s:

$$\delta_T = \frac{1}{h} \sum_{j=1}^{h} \left| \frac{x_{cj} - x_{ej}}{x_{ej}} \right|, \tag{7}$$

where h is the number of samples in the corresponding temperature group.

Quantity δ_{DV} was evaluated for the rate dependence:

$$\delta_{DV} = \frac{1}{m} \sum_{j=1}^{m} \left| \frac{x_{cj} - x_{ej}}{x_{ej}} \right|, \tag{8}$$

where m is the number of samples within range DV.

The following was also calculated for groups of samples with the same growth rate:

$$\delta_V = \frac{1}{k}\sum_{j=1}^{k}\left|\frac{x_{cj} - x_{ej}}{x_{ej}}\right|, \tag{9}$$

where k is the number of samples in the corresponding rate group.

5.2. Chance errors of determination of growth parameters

Even if the model is completely accurate, the values of x_c will deviate from x_e. This is attributable, among other factors, to the errors of determination of molecular flux densities and T_s. The influence of the error of determination of J_{Ga} may be neglected, since the procedure of growth rate measurement and the accuracy of flux density control yield an error $\leq 1\%$ [15,16]. The methods for determination of the flux density of group V molecules and T_s are less accurate [17,18]. In view of this, the probable deviation of x_c from x_e due to inaccuracies of determination of flux densities of group V molecules and T_s was estimated. Model values of proportion of phosphorus x_{c0}, x_{c1}, and x_{c2} were calculated for this purpose at nominal flux densities (J_{0As_2} and J_{0P_2}) and diagonally shifted values ($J_{\max As_2} = J_{0As_2}(1 + 0.055)$ and $J_{\min P_2} = J_{0P_2}(1-0.055)$), and ($J_{\min As_2} = J_{0As_2}(1-0.055)$ and $J_{\max P_2} = J_{0P_2}(1 + 0.055)$), respectively. The substrate temperature was set to T_{s0} (nominal value) in the calculation of x_{c0}. When x_{c1} and x_{c2} were calculated, the magnitude of the absolute error of T_s measurement ($\pm 2.5^\circ$) was added to T_{s0} or subtracted from it so as to maximize the absolute value of residuals $x_{c1}-x_{c0}$ and $x_{c2}-x_{c0}$. The following quantities were then determined:

$$\delta_{c1} = \frac{1}{l}\sum_{j=1}^{l}\left|\frac{x_{c1j} - x_{c0j}}{x_{c0j}}\right|, \tag{10}$$

$$\delta_{c2} = \frac{1}{l}\sum_{j=1}^{l}\left|\frac{x_{c2j} - x_{c0j}}{x_{c0j}}\right|, \tag{11}$$

where l is the number of pairs of J_{0As_2} and J_{0P_2} values. Values from the experimental data set were used for J_{0As_2}, J_{0P_2}, and T_{s0}. The maximum value $\delta_{\max}$ from the (δ_{c1}, δ_{c2}) pair was regarded as the possible greatest relative deviation of x_c from x_e.

5.3. Calculation results

As was already noted, arithmetic mean values δ_{DT} of absolute deviations of x_c from x_e served as the quantitative criterion for evaluation of validity of the model. Table 1 lists δ_{DT} values for several T_s ranges, and δ_T for fixed values of T_s are presented in Table 2. Samples were grown at a rate of ~ 1 MC/c. The values of δ_{DT} and δ_T exceeding $\delta_{\max}$ are highlighted in gray.

Table 3 lists the values of δ_{DV} for different V_g ranges, and deviations for fixed values of V_g at $T_s \sim 500-510^\circ$C are presented in Table 4. The cells highlighted in gray contain such deviations of x_c from x_e that exceed $\delta_{\max}$.

Table 1. Deviation of x_c from x_e within different T_s ranges. $V_g \sim 1$ ML/s

Range of T_s DT, °C	Deviation of x_c from x_e $\delta_{DT} = \frac{1}{p}\sum_{j=1}^{p}\left\|\frac{x_{cj}-x_{ej}}{x_{ej}}\right\|$	$\delta_{\max}$
400−450	0.053	0.109
450−500	0.058	
500−550	0.058	
580−600	0.047	

Table 2. Deviation of x_c from x_e at fixed values of T_s. $V_g \sim 1$ ML/s

T_s, °C	Deviation of x_c from x_e $\delta_T = \frac{1}{h}\sum_{j=1}^{h}\left\|\frac{x_{cj}-x_{ej}}{x_{ej}}\right\|$	$\delta_{\max}$
400	0.052	0.109
410	0.077	
450	0.039	
500	0.062	
550	0.050	
580	0.055	
600	0.039	

Table 3. Deviation of x_c from x_e within different V_g ranges at T_s lying within the interval of 500–510°C

V_g range, ML/s	Deviation of x_c from x_e $\delta_{DV} = \frac{1}{m}\sum_{j=1}^{m}\left\|\frac{x_{cj}-x_{ej}}{x_{ej}}\right\|$	$\delta_{\max}$
0.25−2.20	0.081	0.109
0.25−1.00	**0.121**	
1.00−2.20	0.050	

Table 4. Deviation of x_c from x_e at fixed values of V_g and T_s lying within the interval of 500–510°C

V_g, ML/s	Deviation of x_c from x_e $\delta_V = \frac{1}{k}\sum_{j=1}^{k}\left\|\frac{x_{cj}-x_{ej}}{x_{ej}}\right\|$	$\delta_{\max}$
0.25	**0.211**	0.109
0.50	0.087	
0.98	0.066	
1.01	0.045	
1.38	0.065	
1.98	0.084	
2.20	0.010	

The presented data suggest that expressions (2)−(5) provide an adequate description of the dependence of R_s on the substrate temperature and the flux densities of As_2 and P_2 molecules throughout almost the entire probed range of growth parameters. The identified limitations are discussed below.

6. Discussion

The examined phenomenological approach made it possible to present a discrete and fragmentary set of experimental data in the form of a continuous complex function constructed based on simpler functions with a monotonic behavior within the entire examined range of independent variables (growth parameters). Figure 10 presents the three-dimensional dependence of R_s on $Y = 2J_{As_2}/J_{Ga}$ and $X = 2J_{P_2}/J_{Ga}$ plotted within approximation (2)−(5) at different values of T_S. Two-dimensional dependences of R_s on $2J_{As_2}/J_{Ga}$ and $2J_{P_2}/J_{Ga}$, which are represented by dashed curves in Figs. 4 and 5, correspond to the lines of intersection between surface $R(X, Y, T_s)$ at $T_s = 500°C$ and planes parallel to coordinate planes OYZ and OXZ. It follows from Figs. 3−5 that R_s increases both with $2J_{As_2}/J_{Ga}$ and with $2J_{P_2}/J_{Ga}$. The variation of $2J_{As_2}/J_{Ga}$ has a more significant effect on R_s than the variation of $2J_{P_2}/J_{Ga}$. This agrees qualitatively with the data from [12]. The value of R_s depends only weakly on the magnitude and ratio of molecular fluxes within a certain region of $2J_{As_2}/J_{Ga}$ and $2J_{P_2}/J_{Ga}$ values. At $R_s = 500°C$, this effect is observed when $2J_{As_2}/J_{Ga} > 6$.

It follows from the physical interpretation of expression (1) and the monotonicity of functions governing the behavior of $R_s = R(X, Y, T_s)$ that the composition of a solid solution in the considered implementation of a phenomenological approach is representative of the presence of a certain surface-averaged steady balance of mass transfer processes.

As was already noted, our experimental data on the influence of Ts on x agree qualitatively with the results reported in [13], but contradict the conclusions made in [11], where an increase in substrate temperature led to a reduction in x in the process of epitaxy of a GaP_xAs_{1-x} solid solution from As_4 and P_4 fluxes. This may be attributed to the low rate of layer growth in [11]. According to the model proposed in [14], nonsteady exchange processes in a chemisorbed anion layer (desorption/adsorption) on the terrace surface contribute to the formation of the solid solution composition. Exchange processes alter the anion composition of the terrace surface established in the growth regions localized at the bends of steps. The duration of nonsteady processes is limited by the time of formation of a single monolayer. The lower the growth rate is, the more significant is the composition change outside of growth regions. In turn, the rate constants of exchange processes depend exponentially on substrate temperature. The activation energy of desorption of chemisorbed phosphorus dimers is higher than

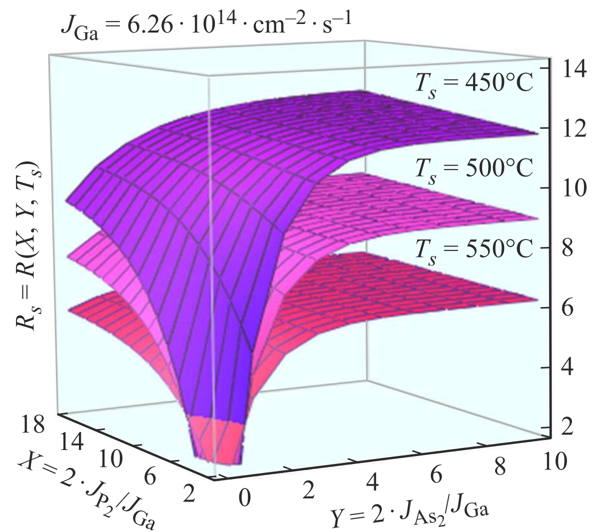

Figure 10. Dependences of R_s on $2J_{As_2}/J_{Ga}$ and $2J_{P_2}/J_{Ga}$ plotted using Eqs. (2)−(5) at different values of T_S.

the activation energy of desorption of chemisorbed arsenic dimers. As T_s grows, the difference between the rate constants of desorption of arsenic and phosphorus dimers decreases. This is evidenced by the S-shaped dependence in Fig. 8. At a growth rate of ~ 1 monolayer per second, this effect manifests itself at $T_S \gtrsim 520°C$. As the growth rate decreases, the S-shaped dependence shifts toward lower T_s values. The value of R_s may increase with increasing T_s at certain combinations of rate constants of exchange processes and the time of formation of a single monolayer.

The obtained expressions provide a fairly accurate description of variation of the composition of a solid solution within almost the entire range of growth parameter values. However, the behavior of R_s in a certain region of values of independent variables cannot be characterized by monotonic functions with the considered number of independent variables. More specifically, this is true at growth rates < 0.5 ML/s. Thus, it appears that the process of formation of the solid solution composition is affected by one more factor that has not been accounted for. The growth rate may be such a factor. The probable influence of the growth rate was discussed in [14].

Note that the degree of relaxation of grown GaP_xAs_{1-x} films varied within a wide range depending on their composition and thickness. However, the variation of the proportion of phosphorus (x) with growth parameters was characterized with a fairly high accuracy.

7. Conclusion

Experimental dependences of the proportion of phosphorus in GaP_xAs_{1-x} films on the conditions of their MBE growth on GaAs(001) substrates from As_2 and P_2 molecular fluxes were characterized using a phenomenological model. Experimental data covering a wide range of epitaxy

parameters were used. Empirical expressions characterizing the dependence of the ratio of incorporation coefficients of arsenic and phosphorus from As_2 and P_2 molecules on the growth conditions were proposed. These expressions allow one to estimate the molecular fluxes of group V elements that provide the needed x value in partially relaxed films of GaP_xAs_{1-x} solid solutions at given values of the substrate temperature and the flux density of gallium atoms. It is of interest to apply the proposed approaches to experimental dependences of the composition in the group V sublattice on the conditions of MBE growth of the entire spectrum of $(A^{III})P_xAs_{1-x}$ solid solutions.

Funding

This study was supported by grant No. 075-15-2020-797 (13.1902.21.0024).

Conflict of interest

The authors declare that they have no conflict of interest.

References

[1] I. Vurgaftmana, J.R. Meyer, L.R. Ram-Mohan. J. Appl. Phys., **89** (11), 5815 (2001).
[2] T. Nishitani, T. Nakanishi, M. Yamamoto, S. Okumi, F. Furuta, M. Miyamoto, M. Kuwahara, N. Yamamoto, K. Naniwa. J. Appl. Phys., **97**, 094907 (2005).
[3] M. Naganuma, K. Takahashi. Phys. Status Solidi A, **31**, 187 (1975).
[4] K. Tateishi, M. Naganuma, K. Takahashi. Jpn. J. Appl. Phys., **15** (5), 785 (1976).
[5] Y. Tatsuoka, H. Kamimoto, Y. Kitano, T. Kitada, S. Shimomura, S. Hiyamizu. J. Vac. Sci. Technol. B, **17** (3), 1155 (1999).
[6] Y. Tatsuoka, H. Kamimoto, T. Kitada, S. Shimomura, S. Hiyamizu. J. Vac. Sci. Technol. B, **18** (3), 1549 (2000).
[7] Y. Tatsuoka, M. Uemura, T. Kitada, S. Shimomura, S. Hiyamizu. J. Cryst. Growth, **227**–**228**, 266 (2001).
[8] H.Q. Hou, B.W. Liang, T.P. Chin, C.W. Tu. Appl. Phys. Lett., **59** (3), 292 (1991).
[9] T.P. Chin, B.W. Liang, H.Q. Hou, M.C. Ho, C.E. Chang, C.W. Tu. Appl. Phys. Lett., **58** (3), 254 (1991).
[10] H.Q. Hou, C.W. Tu. Appl. Phys. Lett., **60**, 1872 (1992).
[11] S. Gonda, Y. Matsushima. Jpn. J. Appl. Phys., **47** (9), 4198 (1976).
[12] C.T. Foxon, B.A. Joyce, M.T. Norris. J. Gryst. Growth, **49**, 132 (1980).
[13] B.W. Liang, C.W. Tu. J. Appl. Phys., **74** (1), 255 (1993).
[14] E.A. Emelyanov, M.A. Putyato, B.R. Semyagin, D.F. Feklin, V.V. Preobrazhensky. Semiconductors, **49** (2), 157 (2015).
[15] J.J. Harris, B.A. Joyce, P.J. Dobson. Surf. Sci., **103**, 90 (1981).
[16] C.E.C. Wood. Surf. Sci., **108**, 441 (1981).
[17] V.V. Preobrazhenskii, V.P. Migal', D.I. Lubyshev. Poverkhn. Fiz., Khim., Mekh., **9**, 156 (1989) (in Russian).
[18] V.V. Preobrazhenskii, M.A. Putyato, B.R. Semyagin. Semiconductors, **36** (8), 837 (2002).

Translated by D.Safin